Differential requirements for Smad4 in TGFβ-dependent patterning of the early mouse embryo

Gerald C. Chu[1,2], N. Ray Dunn[1], Dorian C. Anderson[1], Leif Oxburgh[1] and Elizabeth J. Robertson[1,*]

[1]Department of Molecular and Cellular Biology, Harvard University, Cambridge, MA 02138, USA
[2]Department of Pathology, Brigham and Women's Hospital, Boston, MA 02115, USA
*Author for correspondence (e-mail: ejrobert@fas.harvard.edu)

Accepted 27 April 2004

Development 131, 3501-3512
Published by The Company of Biologists 2004
doi:10.1242/dev.01248

Summary

Genetic and biochemical data have identified Smad4 as a key intracellular effector of the transforming growth factor β (TGFβ) superfamily of secreted ligands. In mouse, *Smad4*-null embryos do not gastrulate, a phenotype consistent with loss of other TGFβ-related signaling components. Chimeric analysis reveals a primary requirement for *Smad4* in the extra-embryonic lineages; however, within the embryo proper, characterization of the specific roles of Smad4 during gastrulation and lineage specification remains limited. We have employed a *Smad4* conditional allele to specifically inactivate the *Smad4* gene in the early mouse epiblast. Loss of *Smad4* in this tissue results in a profound failure to pattern derivatives of the anterior primitive streak, such as prechordal plate, node, notochord and definitive endoderm. In contrast to these focal defects, many well-characterized TGFβ- and Bmp-regulated processes involved in mesoderm formation and patterning are surprisingly unaffected. Mutant embryos form abundant extra-embryonic mesoderm, including allantois, a rudimentary heart and middle primitive streak derivatives such as somites and lateral plate mesoderm. Thus, loss of *Smad4* in the epiblast results not in global developmental abnormalities but instead in restricted patterning defects. These results suggest that Smad4 potentiates a subset of TGFβ-related signals during early embryonic development, but is dispensable for others.

Supplemental data available online

Key words: Smad4, TGFβ, Anterior primitive streak, Mesoderm patterning, Mouse

Introduction

Members of the transforming growth factor β (TGFβ) superfamily of signaling molecules have been implicated in a diverse array of biological processes, including cell growth, differentiation, apoptosis and carcinogenesis (reviewed by Massagué, 1998; Massagué et al., 2000). In the early vertebrate embryo they are indispensable for elaborating the basic body plan and at later stages play a variety of roles during organogenesis and tissue homeostasis. Comprising over 30 different ligands, the superfamily includes TGFβs, activins, nodal, bone morphogenetic proteins (Bmps), and growth and differentiation factors (GDFs). Despite the large number of ligands and their diverse activities, these signals are received and transduced by a relatively small number of cell-surface receptors and downstream effectors.

The receptor complex is composed of two distinct transmembrane serine-threonine kinases termed type I and type II receptors. Upon ligand binding, the activated receptor complex phosphorylates members of the Smad family. The receptor-associated Smads (R-Smads) function as both signal transduction mediators and transcription factors essential for TGFβ signaling and can be subdivided into two groups. While Smad1, Smad5 and Smad8 are phosphorylated in response to Bmp signals, Smad2 and Smad3 are phosphorylated in response to activation of the TGFβ, activin and Nodal pathways. Phosphorylation of the R-Smads allows their association with the common-mediator Smad, Smad4, resulting in nuclear translocation and formation of higher order transcriptional complexes. Current models emphasize the central requirement of Smad4 for the regulation of TGFβ target genes. By itself or in combination with R-Smads, Smad4 weakly binds DNA and only moderately activates transcription. For robust gene activation or suppression, heteromeric Smad4-containing complexes must associate with additional nuclear co-factors or tissue-specific transcription factors such as FoxH1 or OAZ (reviewed by Attisano and Wrana, 2000; Moustakas et al., 2001).

During early vertebrate development, the Nodal signaling pathway plays a conserved role in the establishment of the anteroposterior (AP) axis, gastrulation and left-right patterning (reviewed by Schier, 2003; Whitman, 2001). In the early mouse embryo, Nodal signals from the epiblast are transduced in the overlying visceral endoderm (VE) to establish the early anterior organizer known as the anterior visceral endoderm (AVE) (Lu et al., 2001). The AVE acts prior to gastrulation to impart early anterior character in the adjacent epiblast. *Nodal* mutants fail to pattern the AVE and arrest prior to gastrulation (Brennan et al., 2001). Similarly, null mutations within the Nodal receptor complex, either the type I receptor ALK4 or the type II receptors ActRIIA and ActRIIB, result in embryos that do not gastrulate and overtly resemble *Nodal* mutants (Gu et

al., 1998; Song et al., 1999). Continued Nodal signaling during gastrulation instructs epiblast cells passing through the anterior primitive streak to become definitive endoderm (DE), prechordal plate, node and notochord. Downstream of Nodal signaling, loss of *Smad2* in the epiblast or reducing both *Smad2* and *Smad3* gene dose yield phenotypes indistinguishable from *Nodal* hypomorphic mutations (Dunn et al., 2004; Lowe et al., 2001; Norris et al., 2002; Vincent et al., 2003). Similarly, loss of *Foxh1*, which encodes a forkhead transcription factor that associates with Smad2/3 and Smad4, yields phenotypes that closely resemble those resulting from disruption of the Nodal signaling pathway (Schier, 2003). Taken together, these biochemical and genetic results underscore the significance of the Smad pathway in transducing Nodal signals during early embryogenesis.

Signaling via the Bmp pathway is also crucial in early embryonic development, but loss-of-function phenotypes are much more varied (reviewed by Zhao, 2003). Mutations in the type I receptor *Bmpr1a/Alk3* and type II receptor *Bmpr2* lead to a block prior to gastrulation. Inactivation of *Bmp4* results in a reduction in extra-embryonic mesoderm characterized by a lack of an allantois and loss of primordial germ cells (PGCs) (Lawson et al., 1999). Loss of *Bmp2* and *Bmp8b* also affect allantois development and PGC number (Loebel et al., 2003). Mutations in the Bmp effectors *Smad1* and *Smad5* result in allantois, PGC and yolk sac defects as well as impaired angiogenesis. In addition, genetic analysis has implicated a number of Bmps in heart development including *Bmp2*, *Bmp4*, *Bmp5*, *Bmp6* and *Bmp7*. Compared with the early gastrulation defects associated with Bmp receptor mutations, the phenotypes resulting from loss of individual Bmp ligands or their corresponding downstream Smads are more moderate, perhaps reflecting functional redundancy among Bmp or Smad members.

Consistent with the abundant biochemical data that suggest a central role for Smad4 in the transduction of all TGFβ-related signals, mouse embryos homozygous for a *Smad4* null allele arrest prior to gastrulation (Sirard et al., 1998; Yang et al., 1998). Mutant embryos show disorganization by embryonic day (E) 6.5 and do not form mesoderm, a phenotype more severe than that of any individual R-Smad mutation. Limited analysis of *Smad4*-null embryos indicates that the initial requirement for Smad4 activity resides in the extra-embryonic lineages: aggregation of Smad4-deficient embryonic stem (ES) cells with tetraploid wild-type embryos gives rise to chimeric embryos that express the mesodermal marker *T* and show limited formation of mesodermal derivatives such as somites (Sirard et al., 1998). However, the specific roles of Smad4 within the developing embryo proper have not been well characterized.

We have selectively manipulated *Smad4* gene activity in the epiblast and its derivatives in order to address the combined roles of TGFβ-related signaling during gastrulation and specification of the definitive embryonic lineages. We generated a *Smad4* conditional allele that undergoes efficient Cre-mediated DNA recombination within the epiblast in response to the robust *Sox2Cre* transgene. Loss of Smad4 does not prevent the establishment of the primary AP axis and gastrulation is initiated normally. However, we observe a highly focal defect in patterning of the primitive streak as gastrulation proceeds. Mutant embryos fail to form derivatives of the anterior primitive streak (APS), such as the node, notochord and definitive endoderm, and thus share many phenotypic similarities associated with downregulation of the *Nodal/Smad2/3/Foxh1* pathway. Surprisingly, the transduction of extra-embryonic Bmp signals within the epiblast is only moderately impaired in the absence of *Smad4*. Posterior streak derivatives probably patterned in response to extra-embryonic Bmp signals are induced normally, and mutant embryos consistently form a rudimentary heart tube, yolk sac mesoderm and allantois. By contrast, specification of the germline is *Smad4*-dependent as PGC formation is dramatically diminished. Taken together, these studies indicate that *Smad4* is an essential component of the Nodal signaling pathway that specifies the APS, but is required to transduce only select Bmp signals during early development.

Materials and methods

Generation of Smad4 conditional and null alleles

The *Smad4* conditional ($Smad4^{RobCA}$; referred to throughout as $Smad4^{CA}$) and null ($Smad4^{RobN}$; $Smad4^{N}$) alleles were generated by flanking the first coding exon of *Smad4* with loxP sites (Fig. 1A). The targeting construct contains a pgk-dta selection cassette; a 4.2 kb (*Sal*I-*Stu*I) 5′ homology arm containing a loxP site; a loxP flanked pgk-hygromycin cassette; and a 7.0 Kb (*Stu*I-*Xho*I) 3′ homology arm (Fig. 1A). Linearized vector was electroporated into CCE ES cells, and drug-resistant colonies were genotyped by Southern blot analysis using a 3′ external *Xho*I-*Bst*Z17I probe. Approximately 6% of the clones were correctly targeted. Southern blot analysis was performed using an internal *Stu*I-*Avr*II probe on *Xba*I-digested clones to screen for loss of the pgk-hygromycin cassette and generation of the conditional and exon1-deleted null alleles (Fig. 1C). Two independently targeted ES cell clones were used to generate germ line chimeric mice. In one clone, the pgk-hygromycin cassette was excised by transient expression of Cre-recombinase in vitro; in a second clone, $Smad4^{TA}$ ES cells were used to generate germline chimeric mice. $Smad4^{TA/+}$ mice were bred for in vivo Cre-mediated excision (O'Gorman et al., 1997) of the selection cassette and generation of the $Smad4^{CA}$ and $Smad4^{N}$ alleles. The $Smad4^{CA/CA}$ and $Smad4^{N/N}$ phenotypes obtained from these two ES cell clones are identical.

Genotyping procedures

Mice, ES cells and embryos were genotyped by PCR analysis of cells lysed in buffer containing non-ionic detergents and Proteinase K. Primers used to genotype *Smad4* alleles were F1, 5′-CTTTTA-TTTTCAGATTCAGGGGTTC-3′; F2, 5′-AAAATGGGAAAAC-CAACGAG-3′; and R1, 5′-TACAAGTGCTATGTCTTCAGCG-3′. The combination of the F1, F2 and R1 primers amplifies 512 bp, 625 bp and 675 bp fragments from the $Smad4^{N}$, wild-type and $Smad4^{CA}$ alleles, respectively (Fig. 1A,D).

Mouse strains

$Smad4^{CA/CA}$ was maintained on a (129×C57BL/6) hybrid background. $Smad4^{N/+}$ and $Smad4^{CA/CA}$;$ROSA26^{R/R}$ were maintained on a partially outbred CD1 background. *Sox2Cre*/+;$Smad4^{N/+}$ mice were generated from crosses between $Smad4^{N/+}$ and *Sox2Cre*/+ parents (Hayashi et al., 2002b) and maintained on a CD1 background.

Whole-mount in situ hybridization, X-gal staining, histology and PGC staining

Whole-mount in situ hybridization was performed according to standard procedures (Nagy et al., 2003), with the following commonly available probes *Shh, T, Nodal, Foxa2, Gsc, Hex, Cer1, Otx2, Fgf8, Krox20, Bmp4, Eomes* and *Oct4* (Brennan et al., 2001; Vincent et al., 2003). Additional probes used for this study: *Lim1* (Barnes et al.,

1994), *Mml* (Pearce and Evans, 1999), and *Nkx2.5* and *cardiac alpha-actin* (Norris et al., 2002). X-gal staining was performed as described by Nagy et al. (Nagy et al., 2003). For Hematoxylin and Eosin histology, embryos were processed, sectioned and stained using standard procedures. Histochemical staining of PGCs and mounting of specimens were performed essentially as described (Lawson et al., 1999).

Western blots

ES cells were sonicated in 2× sample buffer containing protease inhibitor cocktail (Roche). Protein extract (40 μg per cell line) was separated on a 10% SDS-PAGE gel and electroblotted onto nitrocellulose (Schleicher & Schuell). The membrane was then hybridized overnight at 4°C with a mouse monoclonal antibody showing affinity for the linker and/or MH2 domain of Smad4 (B-8; Santa Cruz) diluted 1:1000, followed by HRP-conjugated sheep anti-mouse IgG and ECL (Amersham).

Embryoid body differentiation and RT-PCR

Embryoid bodies were generated from ES cell lines (Robertson, 1987), harvested at day 5 of differentiation and then every 2 to 3 days until day 12. RNA was isolated using Absolutely RNA Miniprep Kit (Stratagene). RNA (10 μg) was reverse transcribed using Superscript II RNase H-reverse transcriptase (Invitrogen). For all genes analyzed, cDNA reverse transcribed from 0.1 μg of RNA was used for PCR amplification. PCR amplification was carried out using 1 μCi [α-^{32}P] dCTP per reaction and performed for 22-26 cycles, maintaining linear amplification. The PCR products were separated on a 6% nondenaturing polyacrylamide gel, vacuum dried and subjected to autoradiography. Primer sequences used were as follows: G3PDHF, 5′-ACCACAGTCCATGCCATCAC-3′; G3PDHR, 5′-TCCACCACCCTGTTGCTGTA-3′; Msx1F, 5′-AACCCCTTGCTACACACTTCCTCC-3′; Msx1R, 5′-GGACCACGGATAAATCTCTTGGC-3′; Msx2F, 5′-GGAGCACCGTGGATACAGGAG-3′; Msx2R, 5′-GCACAGGTCTATGGAAGGGGTAG-3′; HnfF, 5′-ATGCCTGCCTCAAAGCCATC-3′; HnfR 5′-CCACTCACACATCTGTCCATTGC-3; TransferrinF, 5′-GCCATCCCATCACAACAAGGTATC-3′; TransferrinR, 5′-CTGCTTCAGATTCTTAGCCCATTC-3′

Isolation of primary embryonic fibroblasts

In order to obtain *Smad4* null murine embryonic fibroblasts (MEFs), we crossed the tamoxifen-inducible Cre transgene *CAGGCre-ER^{TM}* (Hayashi and McMahon, 2002) onto the *Smad4$^{N/+}$* background. Litters of *CAGGCre-ER^{TM};Smad4$^{N/+}$*×*Smad4$^{CA/CA}$* embryos were harvested at E13.5. Embryos were genotyped and fibroblasts were isolated using standard procedures (Nagy et al., 2003). Fibroblasts from *CAGGCre-ER^{TM};Smad4$^{CA/N}$* embryos were pooled as were *Smad4$^{CA/+}$* littermates. Cre recombinase expression was induced by addition of 1 μM 4-OH-Tamoxifen to the culture medium at passage 2. Cells were passaged twice in the presence of 4-OH-Tamoxifen, and seeded for transfection at passage 5. Excision of *Smad4* was verified by PCR genotyping.

Transcriptional reporter assays

Cells were seeded at 3×10^5 cells/well in 12-well dishes prior to transfection with Lipofectamine 2000 (Invitrogen) according to the manufacturer's instructions. The following plasmids (0.75 μg) were used for the 3TP-lux assay: 3TP-lux (Wrana et al., 1992) and pCMV5B-MADR4 (Macías-Silva et al., 1996). For the Msx2-lux assay, 0.5 μg of the following plasmids were used: Msx2-lux (Sirard et al., 2000), pCMV5B-ALK3/HAQD (Hoodless et al., 1996) and pCMV5B-MADR4. Each well was supplemented with 0.25 μg pRL-CMV (Promega) and an empty CMV expression vector was added to bring the total amount of DNA to 1.75 μg/well. Fifteen hours after transfection, growth medium was replaced with serum-free medium with or without 1 nM TGFβ1 (R&D systems). Cell lysates were harvested 30 hours after addition of ligand, and analyzed using the Dual-Luciferase Reporter Assay System (Promega). Mean values of each set of triplicates were plotted as fold induction compared with activation of the reporter in the absence of ligand or constitutively active receptor.

Results

Generation and characterization of a Smad4 conditional allele

Smad4-deficient mouse embryos exhibit arrested growth, failure to express early mesoderm markers and severe disorganization by E7.5 (Sirard et al., 1998; Yang et al., 1998). Tetraploid analysis indicates that these defects reflect a requirement for Smad4 in extra-embryonic lineages. To evaluate more precisely *Smad4* functions during gastrulation, particularly in specification of the definitive embryonic germ layers, we generated a conditional *Smad4* allele (designated *Smad4^{CA}*) using gene targeting to flank the first coding exon of *Smad4* with loxP sites (Fig. 1A-D). ES cells carrying the initial *Smad4* targeted allele (*Smad4^{TA}*) were identified (Fig. 1B), and in vitro expression of Cre recombinase was used to recover derivatives carrying either *Smad4^{CA}* or *Smad4^{N}* (null) alleles (Fig. 1C). *Smad4^{CA}* heterozygous animals were intercrossed to generate stocks of *Smad4^{CA}* homozygotes (Fig. 1D).

As alternate splicing plays a significant role in *Smad4* processing and activity (Pierreux et al., 2000), it was important to confirm that deletion of exon 1 generates a null allele. We generated both *Smad4$^{N/N}$* ES cells by retargeting the remaining wild-type allele in *Smad4$^{N/+}$* ES cells and *Smad4$^{N/N}$* MEFs using a tamoxifen-inducible Cre transgene (Hayashi and McMahon, 2002) and performed functional assays (see Fig. S1 at http://dev.biologists.org/supplemental). Western blot analysis shows that the predominant wild-type 64 kDa *Smad4* protein present in control ES and MEFs is absent in *Smad4$^{N/N}$* cells. Embryoid bodies (EBs) made from *Smad4$^{N/N}$* ES cells were found to have marked downregulation of the visceral endoderm markers *Hnf4* and transferrin and the Bmp-responsive genes *Msx1* and *Msx2*, as described for the previously characterized null *Smad4* allele (Sirard et al., 1998; Sirard et al., 2000). Similarly, transfection assays confirmed that *Smad4$^{N/N}$* MEFs are unresponsive.

Finally, we examined the phenotype of embryos resulting from *Smad4$^{N/+}$* intercrosses. Mutant embryos were grossly identifiable at E6.5 and characterized by a shortened proximodistal axis and thickened endoderm (Fig. 2A,B). Histological analysis showed disorganization of the epiblast and overlying visceral endoderm, with no evidence of mesoderm formation (Fig. 2C,D). This phenotype is indistinguishable from the independently generated *Smad4^{tm1Ari}* and *Smad4^{ex8}* null mutations (Sirard et al., 1998; Yang et al., 1998). Moreover, aged *Smad4$^{N/+}$* heterozygous mice developed gastric tumors, similar to those previously reported (data not shown) (Takaku et al., 1999).

Molecular characterization of Smad4$^{N/N}$ embryos

Both *Smad4$^{N/N}$* and *Nodal*-deficient embryos form a truncated egg cylinder with thickened VE and absence of mesoderm formation. This overt similarity prompted us to characterize *Smad4$^{N/N}$* embryos molecularly. In *Smad4$^{N/N}$* embryos, the pluripotential marker gene *Oct4* is maintained in the epiblast,

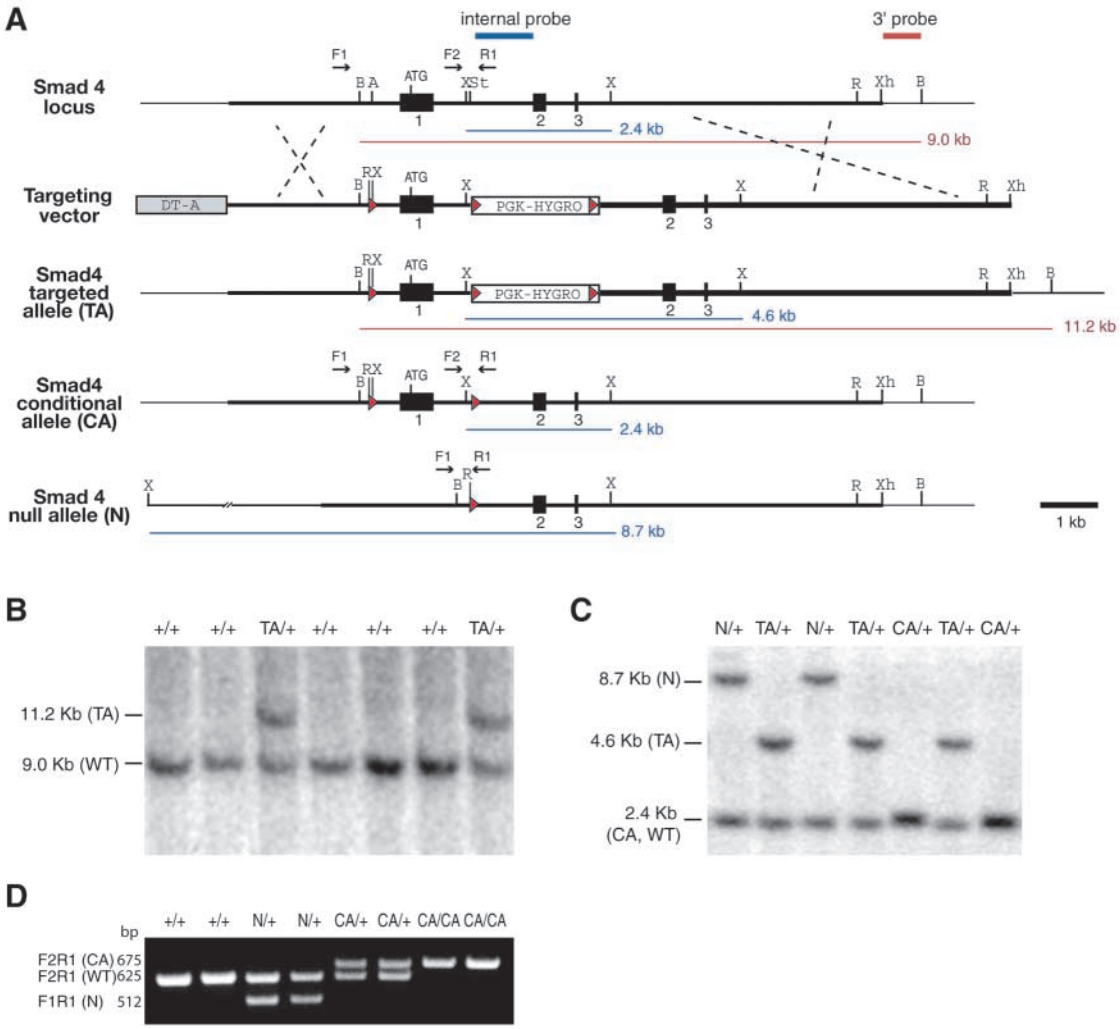

Fig. 1. Generation of *Smad4*^{CA} and *Smad4*^{N} alleles. (A) Strategy used to flank the first coding exon of *Smad4* with loxP sites (red triangles). Targeted clones were identified using a 3′ external probe (red line) and an internal probe (blue line). A, *Apa*I; B, *Bst*Z17I; R, *Eco*RV; St, *Stu*I; X, *Xba*I; Xh, *Xho*I. (B) Southern blot analysis of drug-resistant ES clone DNA digested with *Bst*Z17I and screened using the 3′ external probe yields 9 kb wild-type (WT) and 11.2 kb targeted (TA) alleles. (C) *Smad4*$^{TA/+}$ ES cell clones were transiently transfected with Cre recombinase, and DNA from resultant clones was digested with *Xba*I and screened by Southern blot using the internal probe. Rearrangement of the *Smad4*^{TA} allele generates both *Smad4* conditional (*Smad4*^{CA}) and null (*Smad4*^{N}) alleles. (D) PCR analysis of DNA samples from wild-type, *Smad4*$^{N/+}$, *Smad4*$^{CA/+}$ and *Smad4*$^{CA/CA}$ homozygous mice. PCR primer locations are indicated in A.

in contrast to *Nodal* and *Smad2*$^{-/-}$*; Smad3*$^{-/-}$ double mutants, in which *Oct4* expression is downregulated (Brennan et al., 2001; Dunn et al., 2004). *Bmp4*, a marker of extra-embryonic ectoderm, is expressed in mutants but displaced distally, suggesting disorganization of embryonic and extra-embryonic tissues (Fig. 2G,H). Similarly eomesodermin, which is expressed in extra-embryonic ectoderm and the early primitive streak, shows disorganization along the proximodistal axis (Fig. 2I,J). In *Nodal* mutants, both *Bmp4* and eomesodermin show transient expression which is downregulated by E6.5. Overall, these experiments suggest that although *Smad4*$^{N/N}$ embryos are morphologically similar to *Nodal* mutants, they show a greater degree of axial identity.

Gastrulation occurs in the absence of Smad4 in the epiblast

The failure of *Smad4*-deficient embryos to gastrulate prevents an analysis of the later roles of *Smad4* during embryonic development. To characterize further the requirement of *Smad4* during early gastrulation, we used the *Sox2Cre* deleter strain to specifically inactivate *Smad4* in the epiblast (Hayashi et al., 2002b; Vincent et al., 2003). The *Sox2Cre* transgene exhibits activation in blastocyst outgrowths and is strongly expressed in the early epiblast prior to E5.75 (data not shown). *Sox2Cre* was first introduced into the *Smad4*$^{N/+}$ line of mice, and *Sox2Cre/+;Smad4*$^{N/+}$ and *Smad4*$^{CA/CA}$ animals were subsequently intercrossed. PCR analysis of tissue fragments confirms that rearrangement of the *Smad4* conditional allele efficiently occurs in a Cre- and cell lineage-specific manner (Fig. 3P).

Mutant *Sox2Cre/+;Smad4*$^{CA/N}$ embryos, hereafter designated as *Smad4* mutants, were indistinguishable from control littermates prior to E6.5 (Fig. 3A,A′). At E7.0, mutant embryos have visible anteroposterior (AP) polarity, with

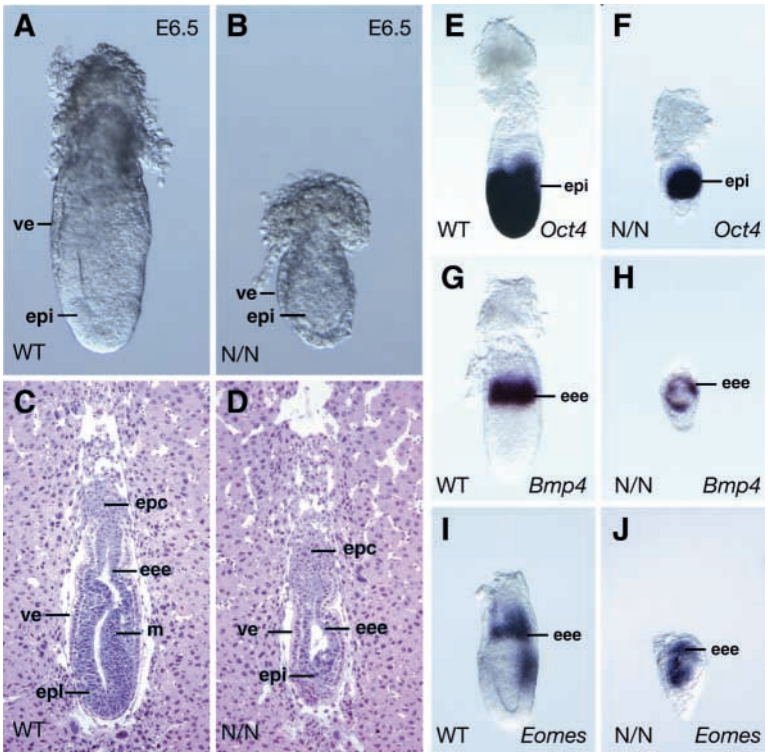

Fig. 2. *Smad4*$^{N/N}$ embryos fail to gastrulate. (A,B) Wild-type (WT) and *Smad4*$^{N/N}$ embryos (N/N) at E6.5. The wild-type embryo displays normal egg cylinder morphology with prominent epiblast (epi) epithelium. By contrast, the mutant embryo (B) shows retarded growth, with circumferential thickening of the visceral endoderm (ve). (C,D) Sagittal sections of E6.5 wild-type and *Smad4*$^{N/N}$ embryos within the deciduum. The wild-type embryo has distinct embryonic and extra-embryonic regions and has begun gastrulation, as evidenced by the formation of posterior mesoderm (m). By contrast, *Smad4*$^{N/N}$ embryos show no mesoderm formation, the visceral endoderm accumulates distally and the epiblast is significantly reduced, with intermingling of extra-embryonic ectoderm (eee). epc, ectoplacental cone. (E-J) Whole-mount in situ hybridization at E6.5 of (E,G,I) wild-type and (F,H,J) *Smad4*$^{N/N}$ mutant embryos. (E,F) *Oct4* is robustly expressed in the epiblast of both mutant and wild-type embryos. (G,I) *Bmp4* and eomesodermin (*Eomes*) expression identifies extra-embryonic ectoderm atop the epiblast. In *Smad4*$^{N/N}$ embryos, this expression domain is displaced distally into the embryonic region (H,J). (I) *Eomes* transcripts also mark the nascent primitive streak in wild-type embryos.

formation of the primitive streak (Fig. 3B,B′). However, as gastrulation proceeds, the AP axis of the embryo is broadened, and by E7.5 and early head fold stages the embryo adopts an elongated and distorted ‘boot-shaped’ morphology (Fig. 3C,C′). In contrast to control littermates, *Smad4* mutants show rudimentary anterior neural development with no visible headfolds and recognizable foregut invagination. At E8.5 mutants reproducibly exhibit a flattened ventral surface with no visible formation of fore- or hindgut, and caudally displaced, bulbous neural tissue (Fig. 3D,D′,E,E′). Somites are formed but are fused across the midline. Other mesodermal derivatives also form in *Smad4* mutants, including allantois, a heart-like structure, blood islands, vasculature and lateral plate mesoderm. By E9.5, mutant embryos show significant degeneration, and none are recovered at E10.5 (data not shown). These results indicate that mesoderm induction in response to Nodal and Bmp pathways does not require Smad4.

Embryos deficient in Smad4 in the epiblast lack anterior primitive streak and axial mesendoderm

To examine axis formation and patterning in more detail, *Smad4* mutants were examined histologically and by whole-mount in situ hybridization. At E7.5, the primitive streak is evident both in cross section and by *T* expression, but is somewhat broadened (Fig. 3J,K, Fig. 4G-J). In wild-type embryos, mesoderm emerges from the primitive streak and migrates anterolaterally between the epiblast and VE. The anterior primitive streak gives rise to a specialized single layer of cells termed the axial mesendoderm (AME) that occupies the ventral midline and marks the point where axial mesoderm and DE converge (Fig. 3H). In *Smad4* mutants, migrating mesoderm traverses the midline without interruption, suggesting loss of AME (Fig. 3I). At E8.5, transverse sections show no evidence of notochord. The neural plate is also flattened and fails to form a tube at any point along the AP axis (Fig. 3M-O).

Our histological analysis reveals that the earliest defects are in the specification of future midline structures, which are derivatives of the APS. We therefore analyzed expression of anterior streak markers in *Smad4* mutants. At E6.5, *Foxa2*, *Gsc* and *Lim1* (*Lhx1* – Mouse Genome Informatics) (Fig. 4A-F) are expressed in the AVE of both wild-type and mutant embryos. This result suggests that specific loss of *Smad4* in the epiblast does not impact the production of epiblast-derived signals that pattern the early anterior organizer. By contrast, *Foxa2*, *Gsc* and *Lim1* expression confined to the APS of wild-type embryos is not observed in *Smad4* mutants.

We next evaluated whether failure to pattern the anterior primitive streak in *Smad4* mutants results in complete loss of its derivatives, the AME, the node and the notochord. At E7.5 the patent node is readily identified by the expression of *Nodal*. In *Smad4* mutant embryos, *Nodal* expression is not observed (Fig. 4M,N). Consistent with this result, *T* and *Shh* transcripts, which also identify the node and anteriorly extending AME, were not detected (Fig. 4I,J,O,P). At E8.5 *T* and *Shh* are additionally expressed in the notochord, but no evidence of a notochord structure is apparent in mutants, although scattered *Shh*-expressing cells are occasionally observed (Fig. 4K,L,Q,R). From these analyses, we conclude that Smad4 in the epiblast functions to specify the APS, and in its absence, midline structures are completely lost.

Smad4 is required for formation of the definitive endoderm

Cell lineage experiments have shown that some of the epiblast cells entering the APS during gastrulation exits and intercalates into the overlying visceral endoderm. These nascent definitive endoderm cells form a sheet that displaces the visceral

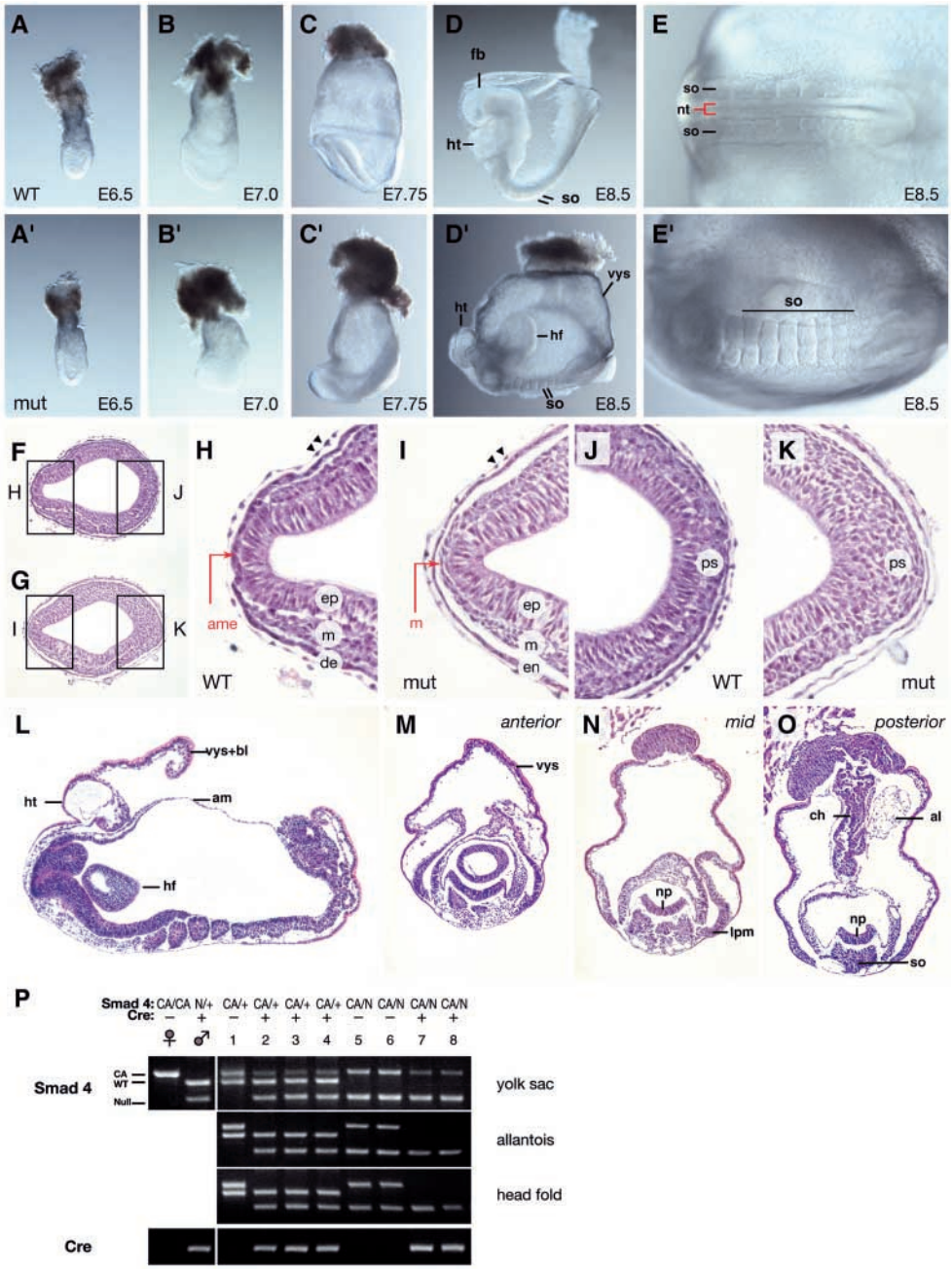

Fig. 3. Loss of *Smad4* from the epiblast disrupts midline formation but does not perturb mesoderm development. (A-E) Developmental time course of (A-E) wild-type (WT) and (A′-E′) *Sox2Cre*;*Smad4*$^{CA/N}$ (mut) embryos. (A,A′) At early gastrulation (E6.5), wild-type and mutant embryos are indistinguishable. (B,B′) By E7.0, mutant embryos have a broadened embryonic region that becomes progressively distorted as development continues. (C,C′) At the early headfold stage (E7.75), anterior elaboration of neural folds and invagination of foregut do not occur in the mutant. (D,D′,E,E′) By E8.5, the mutant embryo has developed within a normal visceral yolk sac (vys). Spherical head fold-like structures appear (hf), a protruding heart (ht)-like structure is observed anteriorly, and somites (so) form, which are fused across the midline. fb, forebrain; nt, neural tube. (F-K) Transverse sections of (F,H,J) wild-type and (G,I,K) E7.5 mutant embryos. (H) Anteriorly, the wild-type embryo shows the normal topological arrangement of the three definitive germ layers: inner anterior ectoderm or epiblast (ep); mesodermal (m) wings; and outer layer of definitive endoderm (de). At the midline, the epiblast directly contacts the axial mesendoderm (ame; red arrow) without an intervening layer of mesoderm. Arrowheads indicate parietal endoderm. (I) In mutant embryos, however, interposing mesoderm (m; red arrow) is observed at the midline, and (J,K) the posterior primitive streak (ps) is broadened compared with the control embryos. (L) Sagittal section of an E8.5 *Sox2Cre/+*;*Smad4*$^{CA/N}$ embryo reveals a rudimentary heart (ht), neural tissue approximating a headfold (hf) as well as visceral yolk sac endoderm with associated blood islands (vys + bl). am, amnion. (M-O) Coronal sections of a similarly staged E8.5 mutant embryo at (M) anterior, (N) mid and (O) posterior levels. The neural plate (np) fails to form the neural tube. Somitic (so) and lateral plate mesoderm (lpm) is seen. Posteriorly, stalk-like chorionic tissue (ch) extends from the amnion and is associated with allantois (al). (P) PCR performed on microdissected tissue fragments of embryos of a *Smad4*$^{CA/CA}$ × *Sox2Cre*;*Smad4*$^{N/+}$ intercross. In embryos expressing the *Sox2Cre* transgene (lanes 2-4, 7, 8), conversion of the conditional allele to the null allele is seen. The yolk sac, which is derived from the epiblast and extra-embryonic endoderm, shows only partial conversion. The epiblast-derived allantois and headfold tissue show complete conditional-to-null conversion.

endoderm proximally and, with the exception of a few residual VE cells, eventually gives rise to the entire embryonic gut (Dufort et al., 1998; Lawson et al., 1991). Chimera studies have uncovered an important requirement for *Foxh1* and *Smad2* in specification of DE progenitors (Hoodless et al., 2001; Tremblay et al., 2000). To investigate whether *Smad4* collaborates with these known components of the Nodal signaling pathway in DE specification, we analyzed expression of *Hex*, which identifies the AVE as well as the earliest population of anterior definite endoderm (ADE) to emerge from the APS (Martinez Barbera et al., 2000; Thomas et al., 1998). At E6.5, the ADE domain of *Hex* expression is absent in *Smad4* mutants (Fig. 5A,B). Consistent with result, at E7.5 *Smad4* mutants fail to activate a *Hex-lacZ* transgene that identifies ADE adjacent to the midline (Fig. 5C-F) (Rodriguez et al., 2001).

The DAN family member *Cer1* provides an additional marker for early DE. In *Smad4* mutants, *Cer1* expression

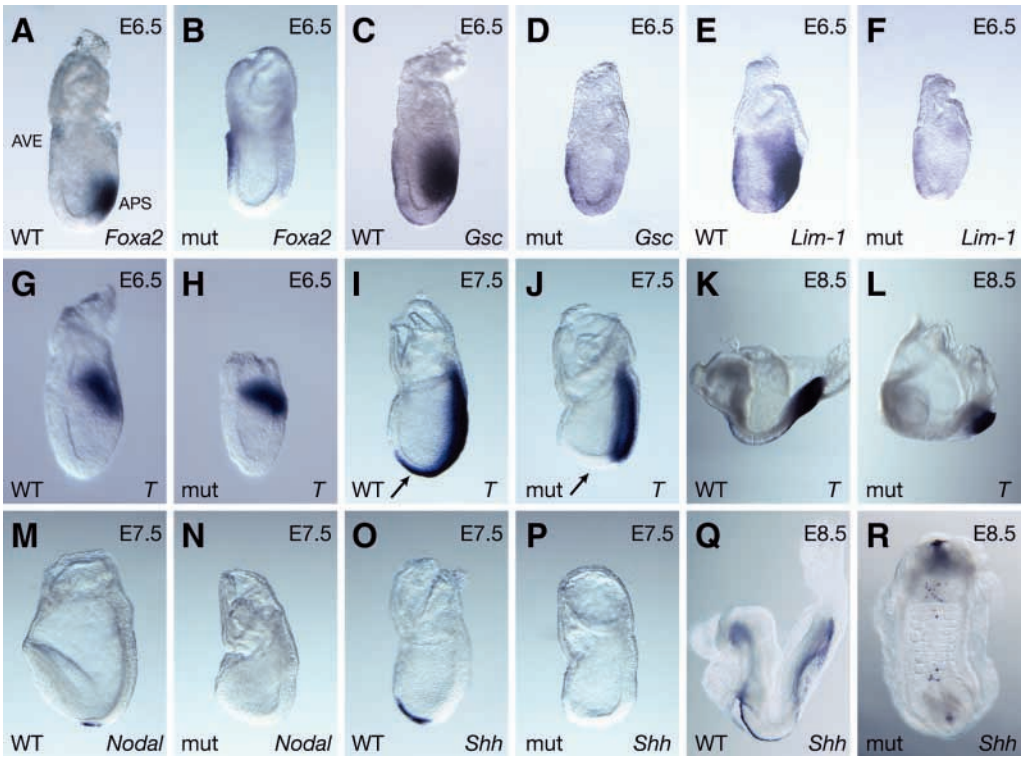

Fig. 4. The anterior primitive streak and its derivatives are absent in *Smad4* mutant embryos. Whole-mount in situ hybridization of (A,C,E,G,I,K,M,O,Q) control and (B,D,F,H,J,L,N,P,R) *Sox2Cre*;*Smad4*$^{CA/N}$ mutants. (A,B) *Foxa2*, (C,D) *Gsc* and (E,F) *Lim1* are expressed in the anterior primitive streak (APS) in wild-type embryos but are absent in mutants. AVE expression is unaffected. (G-L) *T* expression between E6.5 and E8.5. (G,H) At E6.5 *T* expression confirms normal formation of the posterior primitive streak and the initiation of gastrulation. (I,J) By E7.5, *T* expression marks the fully extended primitive streak, and emerging axial mesoderm (arrow). In mutant embryos, no *T*-expressing axial mesoderm is observed. (K,L) Consistent with this result, mutant embryos lack midline expression of *T* in the notochord at E8.5. Posterior *T* transcripts indicate ongoing gastrulation. (M-P) At E7.5, *Nodal* and *Shh* transcripts identify the node, but are absent in mutant embryos. (Q,R) Loss of notochord is further illustrated by the lack of midline *Shh* expression, although some ectopic staining is observed.

in the endoderm is highly reduced, with the extreme anteroproximal domain probably representing residual AVE expression (Fig. 5G,H). In addition, by the late primitive streak stage *Foxa2* extends from the node to the anterior end of the embryo to mark AME derivatives, including DE. In *Smad4* mutants, however, this broad domain of expression is absent (Fig. 5I,J).

To distinguish whether loss of DE markers reflects loss of gene expression or a failure to produce the cells themselves, we performed an in vivo cell lineage assay. The *ROSA26*^{R} conditional allele (Soriano, 1999) was introduced into the *Smad4*^{CA} background. The *Sox2Cre* transgene robustly activates the *ROSA26*^{R} reporter allele in the epiblast. At early headfold stages, the three embryonic lineages – ectoderm, mesoderm and definitive endoderm – comprise exclusively *lacZ*-positive cells, while extra-embryonic tissues are *lacZ* negative (Fig. 5M,N). By contrast, in *Smad4* mutants the superficial endoderm layer is completely devoid of *lacZ* activity, indicating that these cells are extra-embryonic in origin (Fig. 5O,P). This result conclusively shows that Smad4-deficient epiblast cells do not form DE, and consequently the overlying visceral endoderm layer is not displaced.

Anterior neural development in Smad4 mutant embryos

Anterior identity in the mouse is initially specified by the AVE but subsequently reinforced by APS derivatives such as the ADE and prechordal plate. The AVE is normally patterned in *Smad4* mutants and the AP axis is correctly specified. However, mutant embryos fail to form classic headfolds at E7.5 and form a pair of bulbous structures suggestive of rostral CNS at E8.5. We therefore characterized the degree of neural pattern in *Smad4* mutants. *Otx2* is initially expressed in the epiblast and visceral endoderm, but by E7.5 transcripts are restricted to the anterior neurectoderm in both control and mutant embryos (Fig. 6A,B). At E8.5 *Otx2* expression normally resolves to demarcate the forebrain and midbrain. By contrast, expression is confined to the most apical portion of the headfolds in *Smad4* mutants (Fig. 6C,D). A similar reduction was seen in the expression of the forebrain marker *Six3* (Fig. 6E,F). To evaluate anterior CNS defects further, we analyzed *Fgf8* expression, which identifies the anterior neural ridge and the midbrain-hindbrain junction (or isthmus). In *Smad4* mutants, while *Fgf8* is weakly expressed in a region that probably corresponds to the isthmus, the most rostral domain of expression is lost (Fig. 6G,H). Hindbrain patterning was examined using *Krox20* expression, which delineates rhombomeres 3 and 5. Mutant embryos variably exhibit one or two stripes of expression that frequently span the midline (Fig. 6I,J). Collectively, these results suggest that *Smad4* mutants exhibit limited neural patterning, probably imparted by the early activity of the AVE. In the absence of secondary refining signals provided by the anterior AME, the growth and patterning of the neural plate is disrupted.

Bmp-dependent developmental processes are variably affected in the absence of embryonic Smad4

Bmp signaling pathways play evolutionarily conserved roles in heart development. In *Drosophila*, the Bmp homolog

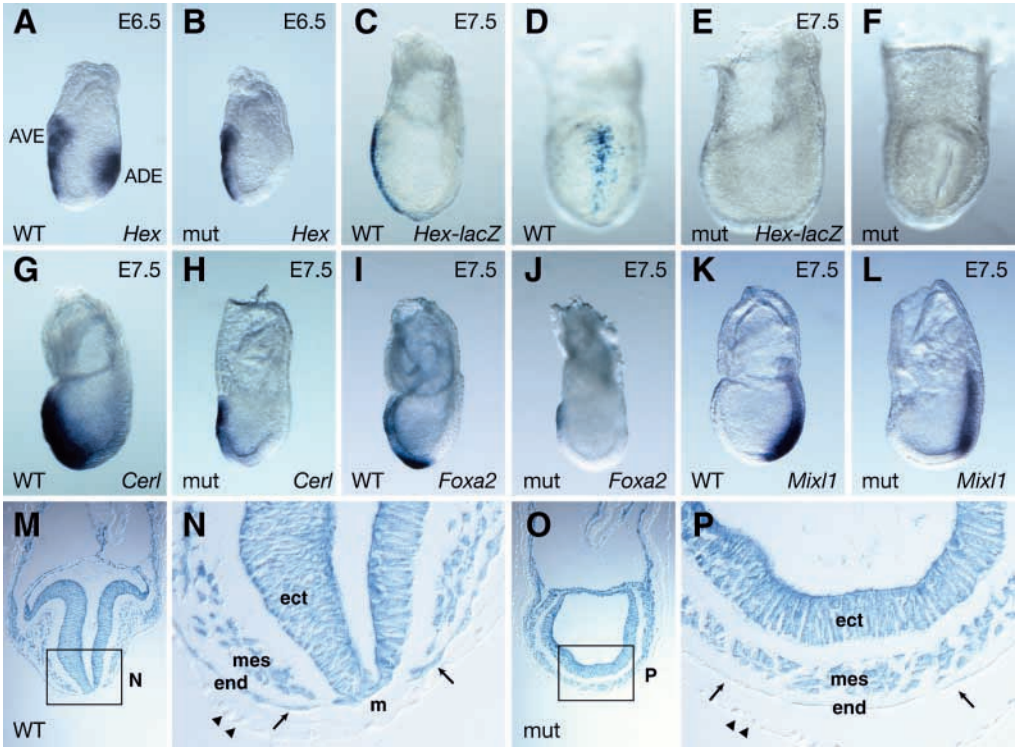

Fig. 5. Definitive endoderm is not formed in *Smad4* mutant embryos. (A,B) *Hex* transcripts mark the anterior visceral endoderm (AVE) and emerging definitive endoderm (DE) at the early primitive streak stage. *Smad4* mutant embryos express *Hex* in the AVE, but not in the ADE. (C-F) A *Hex-lacZ* transgene identifies a portion of medial DE cells (C, lateral view; D, frontal view) at E7.5. By contrast, (E, lateral view; F, frontal view) no transgene activity is detected in mutant embryos. (G,H) *Cerl* expression within the DE shows a drastic reduction in distribution and intensity in mutant embryos, while expression in the AVE is retained. (I,J) At E7.5 *Foxa2* transcripts mark the axial mesendoderm that extends from the anterior streak to the embryonic/extra-embryonic junction. *Smad4* mutant embryos show residual *Foxa2* expression with the AVE but lack axial expression. (K,L) *Mixl1*, a marker of the primitive streak and a putative downstream target of Smad4, is correctly expressed in mutants at the late primitive streak stage. (M-P) *lacZ* expression in (M,N) control and (O,P) *Sox2Cre/+*;*Smad4*$^{CA/N}$;*ROSA26*$^{R/+}$ E7.5 embryos viewed in coronal section. In control embryos, the definitive endoderm layer (arrows) is blue, indicating an epiblast-derived origin. By contrast, this layer is white in mutant embryos, indicating origin from non epiblast-derived visceral endoderm and failure to form DE. Note the absence of midline (m) in mutant embryos. Arrowheads indicate parietal endoderm.

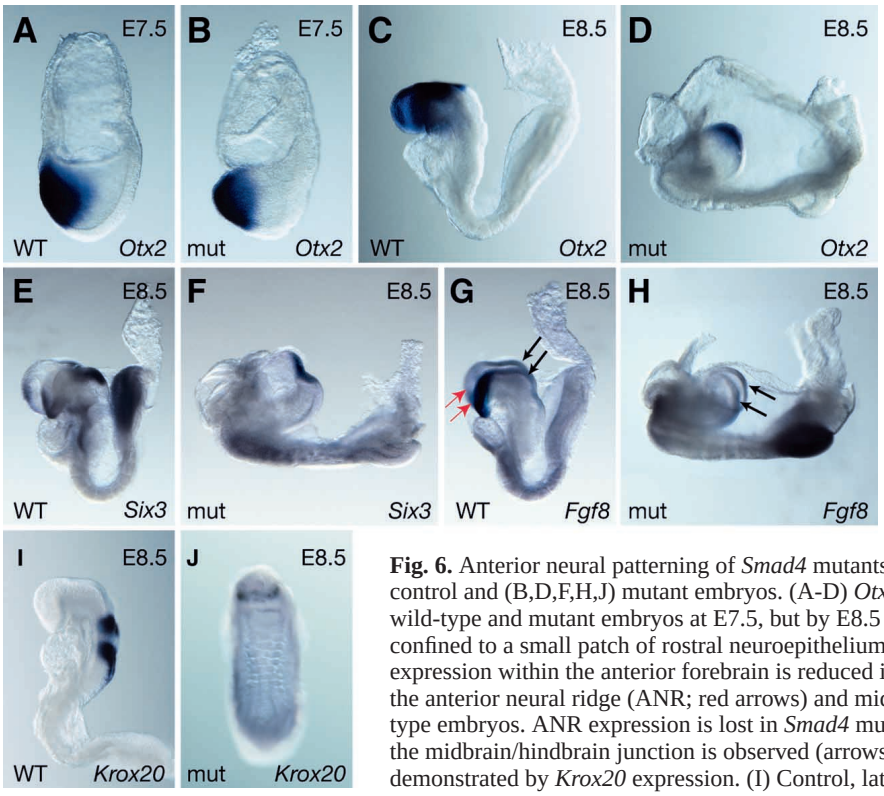

Fig. 6. Anterior neural patterning of *Smad4* mutants. Whole-mount in situ hybridization of (A,C,E,G,I) control and (B,D,F,H,J) mutant embryos. (A-D) *Otx2* expression marks the anterior epiblast of both wild-type and mutant embryos at E7.5, but by E8.5 normal expression within the fore- and midbrain is confined to a small patch of rostral neuroepithelium in *Smad4* mutants. (E,F) Similarly, *Six3* expression within the anterior forebrain is reduced in mutant embryos. (G,H) *Fgf8* transcripts identify the anterior neural ridge (ANR; red arrows) and midbrain/hindbrain junction (black arrows) in wild-type embryos. ANR expression is lost in *Smad4* mutants, while expression probably corresponding to the midbrain/hindbrain junction is observed (arrows). (I,J) Evidence of partial hindbrain formation is demonstrated by *Krox20* expression. (I) Control, lateral view; (J) mutant, ventral view.

Decapentaplegic (Dpp) activates the transcription factor Tinman that specifies contractile cardiomyocytes. In mouse the *Tinman* homolog *Nkx2.5* is one of the earliest markers of cardiogenesis, expressed anteriorly at E7.5 in a crescent-shaped pattern (Fig. 7A,A′). This expression domain is regulated by an enhancer element containing multiple Smad-binding elements (Lien et al., 2002). Intriguingly, *Nkx2.5* expression is unaffected in *Smad4* mutants (Fig. 7B,B′). By E8.5, mutant embryos show consistent formation of a rudimentary heart in the anteriormost part of the embryo (Fig. 7C). Histological analysis reveals a structure with endocardium and cardiomyocyte differentiation, and differentiation of

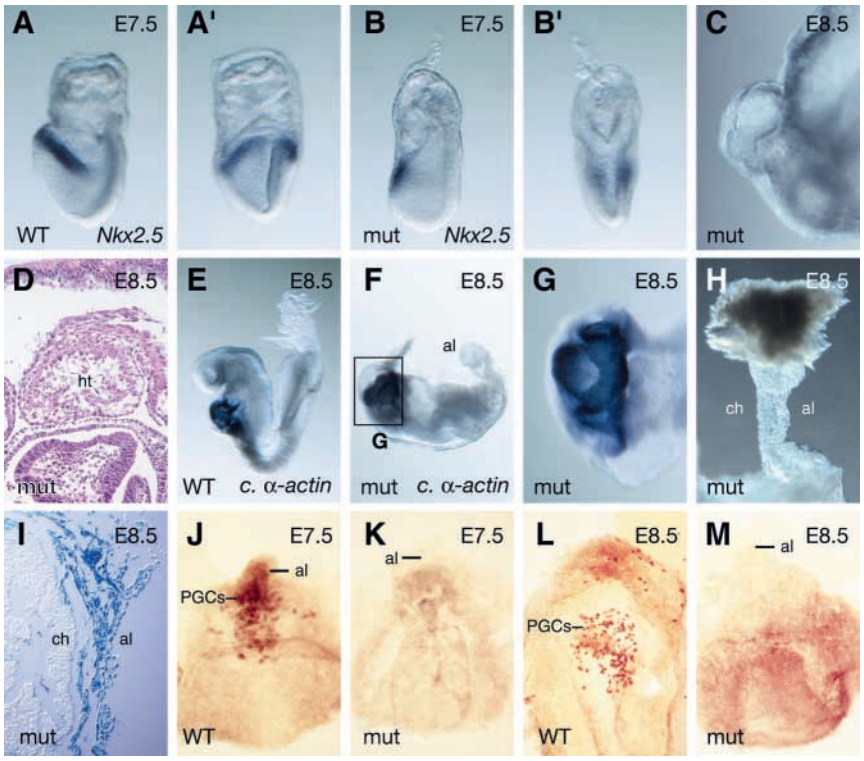

Fig. 7. Several Bmp-dependent developmental processes occur in the absence of embryonic *Smad4*. (A-G) Heart formation in *Smad4* mutant embryos. Specification of the heart field in control (A) and mutant (B) E7.5 embryos as demonstrated by the cardiac marker *Nkx2.5* (A,B, lateral view; A′,B′, anterior view). (C) Higher magnification view of the anterior region of a mutant embryo at E8.5. (D) Coronal section shows heart tube formation with cardiomyocyte differentiation, which is further confirmed by expression of *cardiac alpha actin* at E8.5 (E,F; higher magnification of mutant shown in G). (H,I) The chorion (ch) forms a stalk-like structure often associated with epiblast-derived allantoic mesoderm (al), as shown by *lacZ* expression in *Sox2Cre/+*;*Smad4*$^{CA/N}$;*ROSA26*$^{R/+}$ embryos. (J-M) Alkaline phosphatase (AP) staining for identification of primordial germ cells (PGCs) viewed in flattened tissue preparations. (J) At E7.5, PGCs cluster at the base of the allantois in wild-type embryos. (K) In *Smad4* mutants, PGC formation is not observed. (L) In wild type at E8.5, PGCs begin their anteriorwards migration and intercalate into the hindgut endoderm. (M) Despite formation of allantois, most *Smad4* mutants lack recognizable PGCs at this stage.

cardiac mesoderm is confirmed by cardiac alpha actin expression (Fig. 7D-G). Although the specification of the cardiac lineage occurs in the absence of *Smad4*, development of the heart is abnormal, and at best a primitive unlooped heart tube forms.

Allantois but not primordial germ cells form in Smad4 *mutants*

Recent genetic experiments reveal that null mutations in genes encoding the Bmp2, Bmp4 or Bmp8b ligands or their cognate intracellular effectors Smad1 and Smad5 quantitatively impact primordial germ cell (PGC) formation and variably affect allantois development (McLaren, 2003). These ligands are expressed in either the extra-embryonic ectoderm or visceral endoderm and act prior to gastrulation to predispose a portion of proximal epiblast cells, which express Smad1, Smad5 and Smad8, to the PGC and allantois fates. We therefore evaluated the contribution of *Smad4* to the transduction of extra-embryonic Bmp signals by investigating whether loss of *Smad4* from the epiblast compromises PGC specification and allantois formation.

PGCs can first be identified by their high levels of endogenous alkaline phosphatase (AP) activity around E7.5 and localization in a cluster at the base of the incipient allantois (Fig. 7J). *Smad4* mutants at this stage show disorganized extra-embryonic development, with the collapsing extra-embryonic ectoderm shifted toward the posterior visceral yolk sac. Rudimentary allantois formation is observed in all mutant embryos. However, in the majority of mutants (seven out of nine) no cells resembling PGCs with darkly stained cell membranes or a coarse spot are detected either at the base of the allantois or ectopically within the neighboring visceral yolk sac (Fig. 7K).

To address the possibility that PGC formation is delayed in the absence of *Smad4*, PGC number was assayed one day later at E8.5. In wild-type embryos at this stage, AP-positive PGCs (~100) have dispersed from the base of the allantois and intercalated into the hindgut epithelium (Fig. 7L). All *Smad4* mutants (21 out of 21) show an allantois-like outgrowth that varies in size and that in the majority of cases (70%) associates or fuses with the stalk-like chorionic ectoderm (Fig. 3O, Fig. 7H,I). In the remaining embryos, the allantois terminates blindly within the exocoelomic cavity (Fig. 7F). Despite relatively normal formation of the allantois, the majority of E8.5 mutant embryos (16 out of 21) lack AP-positive PGCs in the posterior extra-embryonic region, including the base of the allantois and visceral yolk sac, or in the posterior embryo proper, which lacks a recognizable hindgut (Fig. 7M). The remaining mutants have fewer than ten PGCs widely scattered in the disorganized posterior region (data not shown). Taken together, these data suggest that *Smad4* is required in the epiblast for specification of the PGC precursor population.

Discussion

We have exploited a conditional allele of *Smad4* to reveal requirements for this gene in the early epiblast. Remarkably, in spite of the well-documented requirements for TGFβ signaling pathways, loss of *Smad4* has a minimal impact on early development. Formation of numerous mesodermal derivatives is unaffected. Rather, our results uncover restricted rules for *Smad4* in the specification of the APS derivatives and in formation of the germline, functions mediated by the Nodal and Bmp pathways, respectively.

Smad4 and formation of the anterior primitive streak

After the onset of gastrulation, inductive events occurring

within the APS are responsible for formation of the node and its derivatives, as well as definitive endoderm. In *Smad4* mutants, these midline structures fail to form, resulting in an embryo with fused somites and anterior defects. The midline defects reflect the inability of the embryo to correctly pattern the APS as seen by failure to activate *Gsc*, *Lim1* and *Foxa2*. The promoter regions of *Gsc* and *Lim1* have been shown to contain activin response elements occupied by a complex containing Smad4, Smad2 and Foxh1 (Labbé et al., 1998; Watanabe et al., 2002), and failure to activate *Gsc* and *Lim1* expression in the APS domain is thus consistent with a essential role for Smad4 in the regulation of these genes.

The definitive endoderm arises from cells within the epiblast that ingress through the APS, displacing the visceral endoderm layer. Our lineage studies and marker analysis indicate that DE is not specified in *Smad4* mutants. As chimeric analysis and conditional gene ablation have also identified a role for *Smad2* and *Foxh1* in endoderm specification, our finding suggests that Smad4 complexes with Smad2/Foxh1 to mediate formation of DE.

Overall, removal of *Smad4* from the epiblast leads to a phenotype that closely resembles that of several other mutants. Embryos in which extra-embryonic lineages are wild-type while the epiblast lacks *Foxa2* fail to form a node and notochord, have fused somites, and establish rudimentary neural patterning (Dufort et al., 1998; Hallonet et al., 2002). *Foxh1* mutant embryos also lack APS derivatives, and show somite fusion (Hoodless et al., 2001; Yamamoto et al., 2001). Removal of *Smad2* alone or in the context of *Smad3* deficiency also leads to similar phenotypes (see below). Collectively, these findings provide genetic evidence that *Smad4*, *Smad2/3* and *Foxh1* lie in the same pathway and support previously characterized biochemical interactions. These mutant contexts each result in downregulation of *Foxa2*, probably accounting for the convergent phenotype. Curiously, no Foxh1/Smad-binding sites have been documented in the *Foxa2* gene, and regulation by Foxh1/Smad proteins may be indirect (Nishizaki et al., 2001).

Smad4 and mesoderm patterning

The central role of Smad4 in transducing TGFβ signals was in part initially characterized by gain-of-function experiments in *Xenopus* embryos. Overexpression of *Smad1* in animal caps simulated the ability of Bmp2 and Bmp4 to induce ventral mesoderm, while *Smad2* induced dorsal mesoderm similar to activin stimulation. As expected, *Smad4* injection produced both dorsal and ventral mesoderm (Lagna et al., 1996; Zhang et al., 1997). These results suggest that *Smad4* contributes essential activities in the events of gastrulation and mesoderm formation. That *Smad4* homozygous null embryos fail to gastrulate was unsurprising, especially in light of similar phenotypes observed in activin/TGFβ and Bmp receptor mutants.

However, when wild-type extra-embryonic lineages are provided either by aggregation of *Smad4*-deficient ES cells with tetraploid wild-type embryos or selective loss of *Smad4* gene activity with *Sox2Cre*, gastrulation commences and mesoderm forms. In *Sox2Cre;Smad4*$^{CA/N}$ mutant embryos, we observe numerous mesodermal derivatives, including somites, heart, allantois and lateral plate mesoderm. We also find that teratomas made from *Smad4*$^{N/N}$ ES cells form mesoderm (G.C.C. and E.J.R., unpublished). These results suggest that the primary defect in *Smad4* homozygous null embryos is restricted to the extra-embryonic lineages. When this requirement is bypassed, *Smad4*-independent gastrulation and mesoderm formation proceeds. Of particular interest, the *Smad4* mutant shows a phenotype less severe than a *Smad2;Smad3* doubly-deficient epiblast (Dunn et al., 2004). Stepwise removal of *Smad2* and *Smad3* from the embryo results in a progressive loss of primitive streak lineages, first impacting APS derivatives such as the AME, node and notochord followed by middle primitive streak lineages such as somites and LPM. The more extensive mesoderm formation seen in *Smad4* mutants therefore suggests that *Smad2* and *Smad3* function in a *Smad4*-independent manner in eliciting *Nodal*-mediated induction of middle streak derivatives. Thus, in the mouse embryo, as in *Xenopus*, *Smad4* appears to potentiate TGFβ signaling to allow the correct patterning of the mesoderm lineage, but *Smad4* activities are unnecessary for mesoderm formation per se.

Initial heart specification does not require Smad4

The role of Bmp-dependent signals in heart formation is evolutionarily conserved. In *Drosophila*, *Dpp* initiates signaling involving the R-Smad *Mad*, the *Smad4* homolog *Medea* and *Tinman*, the homolog of *Nkx2.5*, to specify the cardioblast fate (Zaffran et al., 2002). In chick, a homologous pathway has been described in which Bmp2 or Bmp4 induces expression of *Nkx2.5* in non-cardiogenic mesoderm and directs cardiac differentiation (Schlange et al., 2000; Schultheiss et al., 1997). Intriguingly, we found that removal of *Smad4* in the epiblast affected neither early cardiac development nor correct induction of *Nkx2.5*. Previous promoter analysis identified multiple Smad binding elements in the AR2 enhancer of *Nkx2.5* that governs expression within the cardiac crescent. Mutation of a specific Smad4 binding site leads to complete loss of transgene activity in cardiogenic mesoderm (Lien et al., 2002). Our results therefore suggest that *Smad4* is not essential for activation of the AR2 enhancer and that R-Smad binding and association with other requisite cofactors are sufficient to promote early *Nkx2.5* expression.

Requirement of Smad4 in allantois and PGC development

The Bmp signaling pathway is essential for the normal specification of the mammalian germline (McLaren, 2003). Bmp4 and Bmp8b secreted by the extra-embryonic ectoderm predispose a small number of progenitor cells within the extreme proximal epiblast towards the germ cell fate. Importantly, these precursor cells are multipotent in that they give rise not only to committed PGCs but also to descendants in the extra-embryonic mesoderm, particularly the allantois (Lawson and Hage, 1994). *Bmp4* homozygous null embryos entirely lack PGCs and allantois, whereas heterozygotes show reduced PGC numbers and normal allantois formation (Lawson et al., 1999). Similar gene dose effects are observed in *Bmp8b* mutant embryos (Loebel et al., 2003). These observations suggest that allocation to the germ-cell lineage is more sensitive to the levels of Bmps than is allocation to the allantois. Furthermore, fate mapping studies reveal that the allantois is derived from a much broader region of the proximal epiblast, where Bmp concentrations are expected to be lower, than the narrow belt at the junction with the extra-embryonic

ectoderm in which the common PGC/allantois progenitors reside and which is presumably exposed to the highest local Bmp concentration. The loss of PGCs with persistent formation of allantois in *Smad4* mutant embryos is therefore consistent with the simple model in which Smad4 is required for maximal Bmp signaling within the proximal epiblast, with intermediate signaling reliant upon the available Bmp R-Smads Smad1/5/8 within the epiblast and sufficient for formation of allantois (Hayashi et al., 2002a).

Is Smad4 an obligate member of TGFβ signaling?

The widely held conclusion that *Smad4* occupies a central role in transduction of TGFβ signals comes from multiple lines of biochemical and genetic evidence (reviewed by Massagué, 1998). *Smad4* participates in both activin and Bmp pathways as demonstrated in *Xenopus* overexpression assays and in dominant-negative experiments. In reconstitution experiments, cell lines that lack *Smad4* fail to respond to TGFβ signals; transfection of wild-type *Smad4* restores the signaling capabilities of these cells (de Caestecker et al., 1997; Lagna et al., 1996; Zhang et al., 1997). Moreover, in *Drosophila*, *Medea/Smad4* is necessary for *Dpp* function, and elimination of maternal and zygotic *Medea* in the embryo results in dorsoventral patterning defects identical to that of null *Dpp* mutants, indicating that *Medea* is required for *Dpp*-dependent signaling (Das et al., 1998; Hudson et al., 1998).

By contrast, our data suggest that in the early embryo, *Smad4* is required for certain TGFβ/Bmp signaling pathways, but not obligate for others. A growing body of data corroborates our observations. For example, in *Smad4*-deficient MEFs as well as several *Smad4*-deficient human tumor cell lines, TGFβ addition still results in classical growth inhibition (reviewed by Derynck and Zhang, 2003; Wakefield and Roberts, 2002). In *Drosophila*, oogenesis is more severely disrupted by the loss of the R-Smad *Mad* than by *Medea*. Interestingly, in wing imaginal discs, loss of *Medea* most severely affects regions receiving low *Dpp* signal (Wisotzkey et al., 1998). One possible explanation is that *Medea* normally potentiates weak *Dpp* signals and that in the absence of *Medea*, R-Smads regulate target genes only when the *Dpp* signal strength is high. R-Smads may substitute for or bypass the requirement for Smad4, resulting in unpotentiated levels of downstream signal (Yeo et al., 1999). Additionally, alternate TGFβ pathways have been described, including the Ras/Mapk, Pp2a/S6 kinase, Rhoa and PI3K-Akt pathways, some of which are entirely Smad independent and others that involve crosstalk with Smad signals. Finally, an independently-derived *Smad4* conditional allele was recently employed to eliminate *Smad4* function during CNS and mammary gland development and the resulting phenotypes were surprisingly mild (Li et al., 2003; Zhou et al., 2003). These findings in combination with our genetic results emphasize the versatility in the intracellular transduction of TGFβ-related signals, and encourage a more careful consideration of the current canonical model of TGFβ signaling that places Smad4 as a central effector molecule.

We are grateful to Elizabeth Bikoff for insightful comments and to Cindy Lu for review of the manuscript. We thank Shigemi Hayashi and Andrew McMahon for providing the *Cre-ER*^{TM} and *Sox2Cre* mice, Tristan Rodriguez for *Hex-lacZ* mice, Phil Soriano for *ROSA26*^{R} mice, and Makoto Taketo for *Smad4* genomic constructs. We also thank Joan Massagué, Robert Maxson, Jonathan Pearce and Christian Sirard for plasmid reagents and probes. G.C.C. was supported by the Howard Hughes Medical Institute Postdoctoral Fellowship for Physicians, N.R.D. by a postdoctoral fellowship from the NICHD, and L.O. by a fellowship from the Wenner-Gren Foundations. This work was supported by a grant from the NIH to E.J.R.

References

Attisano, L. and Wrana, J. L. (2000). Smads as transcriptional co-modulators. *Curr. Opin. Cell Biol.* **12**, 235-243.

Barnes, J. D., Crosby, J. L., Jones, C. M., Wright, C. V. and Hogan, B. L. (1994). Embryonic expression of Lim-1, the mouse homolog of *Xenopus* Xlim-1, suggests a role in lateral mesoderm differentiation and neurogenesis. *Dev. Biol.* **161**, 168-178.

Brennan, J., Lu, C. C., Norris, D. P., Rodriguez, T. A., Beddington, R. S. and Robertson, E. J. (2001). Nodal signalling in the epiblast patterns the early mouse embryo. *Nature* **411**, 965-969.

Das, P., Maduzia, L. L., Wang, H., Finelli, A. L., Cho, S. H., Smith, M. M. and Padgett, R. W. (1998). The *Drosophila* gene Medea demonstrates the requirement for different classes of Smads in dpp signaling. *Development* **125**, 1519-1528.

de Caestecker, M. P., Hemmati, P., Larisch-Bloch, S., Ajmera, R., Roberts, A. B. and Lechleider, R. J. (1997). Characterization of functional domains within Smad4/DPC4. *J. Biol. Chem.* **272**, 13690-13696.

Derynck, R. and Zhang, Y. E. (2003). Smad-dependent and Smad-independent pathways in TGF-beta family signalling. *Nature* **425**, 577-584.

Dufort, D., Schwartz, L., Harpal, K. and Rossant, J. (1998). The transcription factor HNF3beta is required in visceral endoderm for normal primitive streak morphogenesis. *Development* **125**, 3015-3025.

Dunn, N. R., Vincent, S. D., Oxburgh, L., Robertson, E. J. and Bikoff, E. K. (2004). Combinatorial activities of Smad2 and Smad3 regulate mesoderm formation and patterning in the mouse embryo. *Development* **131**, 1717-1728.

Gu, Z., Nomura, M., Simpson, B. B., Lei, H., Feijen, A., van den Eijnden-van Raaij, J., Donahoe, P. K. and Li, E. (1998). The type I activin receptor ActRIB is required for egg cylinder organization and gastrulation in the mouse. *Genes Dev.* **12**, 844-857.

Hallonet, M., Kaestner, K. H., Martin-Parras, L., Sasaki, H., Betz, U. A. and Ang, S. L. (2002). Maintenance of the specification of the anterior definitive endoderm and forebrain depends on the axial mesendoderm: a study using HNF3beta/Foxa2 conditional mutants. *Dev. Biol.* **243**, 20-33.

Hayashi, S. and McMahon, A. P. (2002). Efficient recombination in diverse tissues by a tamoxifen-inducible form of Cre: a tool for temporally regulated gene activation/inactivation in the mouse. *Dev. Biol.* **244**, 305-318.

Hayashi, K., Kobayashi, T., Umino, T., Goitsuka, R., Matsui, Y. and Kitamura, D. (2002a). SMAD1 signaling is critical for initial commitment of germ cell lineage from mouse epiblast. *Mech. Dev.* **118**, 99-109.

Hayashi, S., Lewis, P., Pevny, L. and McMahon, A. P. (2002b). Efficient gene modulation in mouse epiblast using a Sox2Cre transgenic mouse strain. *Gene Expr. Patterns* **2**, 93-97.

Hoodless, P. A., Haerry, T., Abdollah, S., Stapleton, M., O'Connor, M. B., Attisano, L. and Wrana, J. L. (1996). MADR1, a MAD-related protein that functions in BMP2 signaling pathways. *Cell* **85**, 489-500.

Hoodless, P. A., Pye, M., Chazaud, C., Labbe, E., Attisano, L., Rossant, J. and Wrana, J. L. (2001). FoxH1 (Fast) functions to specify the anterior primitive streak in the mouse. *Genes Dev.* **15**, 1257-1271.

Hudson, J. B., Podos, S. D., Keith, K., Simpson, S. L. and Ferguson, E. L. (1998). The *Drosophila* Medea gene is required downstream of dpp and encodes a functional homolog of human Smad4. *Development* **125**, 1407-1420.

Labbé, E., Silvestri, C., Hoodless, P. A., Wrana, J. L. and Attisano, L. (1998). Smad2 and Smad3 positively and negatively regulate TGF beta-dependent transcription through the forkhead DNA-binding protein FAST2. *Mol. Cell* **2**, 109-120.

Lagna, G., Hata, A., Hemmati-Brivanlou, A. and Massague, J. (1996). Partnership between DPC4 and SMAD proteins in TGF-beta signalling pathways. *Nature* **383**, 832-836.

Lawson, K. A. and Hage, W. J. (1994). Clonal analysis of the origin of primordial germ cells in the mouse. *CIBA Found. Symp.* **182**, 68-84.

Lawson, K. A., Meneses, J. J. and Pedersen, R. A. (1991). Clonal analysis of epiblast fate during germ layer formation in the mouse embryo. *Development* **113**, 891-911.

Lawson, K. A., Dunn, N. R., Roelen, B. A., Zeinstra, L. M., Davis, A. M., Wright, C. V. E., Korving, J. P. and Hogan, B. L. M. (1999). Bmp4 is required for the generation of primordial germ cells in the mouse embryo. *Genes Dev.* **13**, 424-436.

Li, W., Qiao, W., Chen, L., Xu, X., Yang, X., Li, D., Li, C., Brodie, S. G., Meguid, M. M., Hennighausen, L. et al. (2003). Squamous cell carcinoma and mammary abscess formation through squamous metaplasia in Smad4/Dpc4 conditional knockout mice. *Development* **130**, 6143-6153.

Lien, C. L., McAnally, J., Richardson, J. A. and Olson, E. N. (2002). Cardiac-specific activity of an Nkx2-5 enhancer requires an evolutionarily conserved Smad binding site. *Dev. Biol.* **244**, 257-266.

Loebel, D. A., Watson, C. M., De Young, R. A. and Tam, P. P. (2003). Lineage choice and differentiation in mouse embryos and embryonic stem cells. *Dev. Biol.* **264**, 1-14.

Lowe, L. A., Yamada, S. and Kuehn, M. R. (2001). Genetic dissection of nodal function in patterning the mouse embryo. *Development* **128**, 1831-1843.

Lu, C. C., Brennan, J. and Robertson, E. J. (2001). From fertilization to gastrulation: axis formation in the mouse embryo. *Curr. Opin. Genet. Dev.* **11**, 384-392.

Macías-Silva, M., Abdollah, S., Hoodless, P. A., Pirone, R., Attisano, L. and Wrana, J. L. (1996). MADR2 is a substrate of the TGFbeta receptor and its phosphorylation is required for nuclear accumulation and signaling. *Cell* **87**, 1215-1224.

Martinez Barbera, J. P., Clements, M., Thomas, P., Rodriguez, T., Meloy, D., Kioussis, D. and Beddington, R. S. P. (2000). The homeobox gene Hex is required in definitive endodermal tissues for normal forebrain, liver and thyroid formation. *Development* **127**, 2433-2445.

Massagué, J. (1998). TGF-beta signal transduction. *Annu. Rev. Biochem.* **67**, 753-791.

Massagué, J., Blain, S. W. and Lo, R. S. (2000). TGFbeta signaling in growth control, cancer, and heritable disorders. *Cell* **103**, 295-309.

McLaren, A. (2003). Primordial germ cells in the mouse. *Dev. Biol.* **262**, 1-15.

Moustakas, A., Souchelnytskyi, S. and Heldin, C. H. (2001). Smad regulation in TGF-beta signal transduction. *J. Cell Sci.* **114**, 4359-4369.

Nagy, A., Gertsenstein, M., Vintersten, K. and Behringer, R. (2003). *Manipulating the Mouse Embryo: A Laboratory Manual*. New York, NY: Cold Spring Harbor Laboratory Press.

Nishizaki, Y., Shimazu, K., Kondoh, H. and Sasaki, H. (2001). Identification of essential sequence motifs in the node/notochord enhancer of Foxa2 (Hnf3beta) gene that are conserved across vertebrate species. *Mech. Dev.* **102**, 57-66.

Norris, D. P., Brennan, J., Bikoff, E. K. and Robertson, E. J. (2002). The Foxh1-dependent autoregulatory enhancer controls the level of Nodal signals in the mouse embryo. *Development* **129**, 3455-3468.

O'Gorman, S., Dagenais, N. A., Qian, M. and Marchuk, Y. (1997). Protamine-Cre recombinase transgenes efficiently recombine target sequences in the male germ line of mice, but not in embryonic stem cells. *Proc. Natl. Acad. Sci. USA* **94**, 14602-14607.

Pearce, J. J. and Evans, M. J. (1999). Mml, a mouse Mix-like gene expressed in the primitive streak. *Mech. Dev.* **87**, 189-192.

Pierreux, C. E., Nicolas, F. J. and Hill, C. S. (2000). Transforming growth factor beta-independent shuttling of Smad4 between the cytoplasm and nucleus. *Mol. Cell. Biol.* **20**, 9041-9054.

Robertson, E. J. (1987). Embryo-derived stem cell lines. In *Teratocarcinoma and Embryonic Stem Cells: A Practical Approach* (ed. E. J. Robertson), pp. 71-112. Oxford, UK: IRL Press.

Rodriguez, T. A., Casey, E. S., Harland, R. M., Smith, J. C. and Beddington, R. S. (2001). Distinct enhancer elements control Hex expression during gastrulation and early organogenesis. *Dev. Biol.* **234**, 304-316.

Schier, A. F. (2003). Nodal signaling in vertebrate development. *Annu. Rev. Cell Dev. Biol.* **19**, 589-621.

Schlange, T., Andree, B., Arnold, H. H. and Brand, T. (2000). BMP2 is required for early heart development during a distinct time period. *Mech. Dev.* **91**, 259-270.

Schultheiss, T. M., Burch, J. B. and Lassar, A. B. (1997). A role for bone morphogenetic proteins in the induction of cardiac myogenesis. *Genes Dev.* **11**, 451-462.

Sirard, C., de la Pompa, J. L., Elia, A., Itie, A., Mirtsos, C., Cheung, A., Hahn, S., Wakeham, A., Schwartz, L., Kern, S. E. et al. (1998). The tumor suppressor gene Smad4/Dpc4 is required for gastrulation and later for anterior development of the mouse embryo. *Genes Dev.* **12**, 107-119.

Sirard, C., Kim, S., Mirtsos, C., Tadich, P., Hoodless, P. A., Itie, A., Maxson, R., Wrana, J. L. and Mak, T. W. (2000). Targeted disruption in murine cells reveals variable requirement for Smad4 in transforming growth factor beta-related signaling. *J. Biol. Chem.* **275**, 2063-2070.

Song, J., Oh, S. P., Schrewe, H., Nomura, M., Lei, H., Okano, M., Gridley, T. and Li, E. (1999). The type II activin receptors are essential for egg cylinder growth, gastrulation, and rostral head development in mice. *Dev. Biol.* **213**, 157-169.

Soriano, P. (1999). Generalized lacZ expression with the ROSA26 Cre reporter strain. *Nat. Genet.* **21**, 70-71.

Takaku, K., Miyoshi, H., Matsunaga, A., Oshima, M., Sasaki, N. and Taketo, M. M. (1999). Gastric and duodenal polyps in Smad4 (Dpc4) knockout mice. *Cancer Res.* **59**, 6113-6117.

Thomas, P. Q., Brown, A. and Beddington, R. S. P. (1998). Hex: a homeobox gene revealing peri-implantation asymmetry in the mouse embryo and an early transient marker of endothelial cell precursors. *Development* **125**, 85-94.

Tremblay, K. D., Hoodless, P. A., Bikoff, E. K. and Robertson, E. J. (2000). Formation of the definitive endoderm in mouse is a Smad2-dependent process. *Development* **127**, 3079-3090.

Vincent, S. D., Dunn, N. R., Hayashi, S., Norris, D. P. and Robertson, E. J. (2003). Cell fate decisions within the mouse organizer are governed by graded Nodal signals. *Genes Dev.* **17**, 1646-1662.

Wakefield, L. M. and Roberts, A. B. (2002). TGF-beta signaling: positive and negative effects on tumorigenesis. *Curr. Opin. Genet. Dev.* **12**, 22-29.

Watanabe, M., Rebbert, M. L., Andreazzoli, M., Takahashi, N., Toyama, R., Zimmerman, S., Whitman, M. and Dawid, I. B. (2002). Regulation of the Lim-1 gene is mediated through conserved FAST-1/FoxH1 sites in the first intron. *Dev. Dyn.* **225**, 448-456.

Whitman, M. (2001). Nodal signaling in early vertebrate embryos: themes and variations. *Dev. Cell* **1**, 605-617.

Wisotzkey, R. G., Mehra, A., Sutherland, D. J., Dobens, L. L., Liu, X., Dohrmann, C., Attisano, L. and Raftery, L. A. (1998). Medea is a *Drosophila* Smad4 homolog that is differentially required to potentiate DPP responses. *Development* **125**, 1433-1445.

Wrana, J. L., Attisano, L., Carcamo, J., Zentella, A., Doody, J., Laiho, M., Wang, X. F. and Massague, J. (1992). TGF beta signals through a heteromeric protein kinase receptor complex. *Cell* **71**, 1003-1014.

Yamamoto, M., Meno, C., Sakai, Y., Shiratori, H., Mochida, K., Ikawa, Y., Saijoh, Y. and Hamada, H. (2001). The transcription factor FoxH1 (FAST) mediates nodal signaling during anterior-posterior patterning and node formation in the mouse. *Genes Dev.* **15**, 1242-1256.

Yang, X., Li, C., Xu, X. and Deng, C. (1998). The tumor suppressor SMAD4/DPC4 is essential for epiblast proliferation and mesoderm induction in mice. *Proc. Natl. Acad. Sci. USA* **95**, 3667-3672.

Yeo, C. Y., Chen, X. and Whitman, M. (1999). The role of FAST-1 and Smads in transcriptional regulation by activin during early *Xenopus* embryogenesis. *J. Biol. Chem.* **274**, 26584-26590.

Zaffran, S., Xu, X., Lo, P. C., Lee, H. H. and Frasch, M. (2002). Cardiogenesis in the *Drosophila* model: control mechanisms during early induction and diversification of cardiac progenitors. *Cold Spring Harb. Symp. Quant. Biol.* **67**, 1-12.

Zhang, Y., Musci, T. and Derynck, R. (1997). The tumor suppressor Smad4/DPC 4 as a central mediator of Smad function. *Curr. Biol.* **7**, 270-276.

Zhao, G. Q. (2003). Consequences of knocking out BMP signaling in the mouse. *Genesis* **35**, 43-56.

Zhou, Y. X., Zhao, M., Li, D., Shimazu, K., Sakata, K., Deng, C. X. and Lu, B. (2003). Cerebellar deficits and hyperactivity in mice lacking Smad4. *J. Biol. Chem.* **278**, 42313-42320.